

Anthropogenic control over wintertime oxidation of atmospheric pollutants

J.D. Haskins,¹ F.D. Lopez-Hilfiker,^{1†} B. H. Lee,¹ V. Shaw,^{1††} G. M. Wolfe,^{2,3} J. DiGangi,⁴ D. Fibiger,^{5,13 †††} E.E. McDuffie,^{5,6,13 ‡} P. Veres,⁵ J.C. Schroder,^{5,6} P. Campuzano-Jost,^{5,6} D.A. Day,^{5,6} J. Jimenez,^{5,6} A. Weinheimer,⁷ T. Sparks,⁸ C. Ebben,⁸ R. C. Cohen,⁸ T. Campos,⁷ A. Sullivan,⁹ H. Guo,¹⁰ R. Weber,¹⁰ J. Dibb,¹¹ J. Greene,¹² M. Fiddler,¹² S. Bililign,¹² L. Jaegle,¹ S.S. Brown,^{7,13} J.A. Thornton^{1*}

¹ Department of Atmospheric Sciences, University of Washington, Seattle, WA USA

² Joint Center for Earth Systems Technology, University of Maryland Baltimore County, Baltimore, MD USA

³ Atmospheric Chemistry and Dynamics Laboratory, NASA Goddard Space Flight Center, Greenbelt, MD USA

⁴ NASA Langley Research Center, Hampton, VA USA

⁵ Cooperative Institute for Research in Environmental Sciences, University of Colorado, Boulder, CO, USA

⁶ Department of Chemistry, University of Colorado, Boulder, CO USA

⁷ Earth Observing Laboratory, National Center for Atmospheric Research, Boulder, CO USA

⁸ Department of Chemistry, University of California, Berkeley CA USA

⁹ Department of Atmospheric Sciences, Colorado State University, Fort Collins, CO USA

¹⁰ School of Earth and Atmospheric Sciences, Georgia Institute of Technology, Atlanta, GA USA

¹¹ Department of Earth Sciences, University of New Hampshire, Durham, NH USA

¹² Department of Physics, North Carolina A&T State University, Greensboro, NC USA

¹³ Chemical Sciences Division, NOAA Earth System Research Laboratory, Boulder, CO USA

† Now at Tofwerk AG, Switzerland

†† Now at Harvard University, Cambridge, USA

††† Now at California Air Resources Board, Sacramento, USA

‡ Now at the Department of Physics and Atmospheric Science, Dalhousie University, Halifax, NS, Canada

* Correspondence to: thornton@atmos.washington.edu

50 **Anthropogenic air pollutants such as nitrogen oxides (NO_x = NO + NO₂), sulfur dioxide (SO₂),**
51 **and volatile organic compounds (VOC), among others, are emitted to the atmosphere**
52 **throughout the year from energy production and use, transportation, and agriculture. These**
53 **primary pollutants lead to the formation of secondary pollutants such as fine particulate**
54 **matter (PM_{2.5}) and ozone (O₃) [Seinfeld, 1989; Dabdub et al., 1997; Jacobson et al., 2000;**
55 **Volkamer et al., 2006;], as well as to acid and nutrient deposition to ecosystems [Schofield,**
56 **1976; Irwin et al., 1988; Menz et al., 2004; Greaver et al., 2012;] and perturbations to the**
57 **abundance and lifetimes of short-lived greenhouse gases [Wang et al., 1976; Fishman et al.,**
58 **1980; Jacob & Winner, 2009; Ramanathan et al., 2009;]. Free radical oxidation reactions**
59 **driven by solar radiation govern the atmospheric lifetimes and transformations of most**
60 **primary pollutants and thus their spatial distributions [Weinstock, 1969; Levy, 1971; Seinfeld,**
61 **1989; Collins et al., 2002;]. During winter in the mid and high latitudes, where a large fraction**
62 **of atmospheric pollutants are emitted globally, such photochemical oxidation is significantly**
63 **slower [Levy et al., 1985; Klonecki & Levy, 1997; Yienger et al., 1999]. Using observations**
64 **from a highly instrumented aircraft, we show that multi-phase reactions between gas-phase**
65 **NO_x reservoirs and aerosol particles, as well as VOC emissions from anthropogenic activities,**
66 **lead to a suite of atypical radical precursors dominating the oxidizing capacity in polluted**
67 **winter air, and thus, the distribution and fate of primary pollutants on a regional to global**
68 **scale.**

69
70 In the warmer and more photochemically active summer months, the photolysis of ozone (O₃) in
71 the presence of water vapor leads to production of hydroxyl radicals (OH).

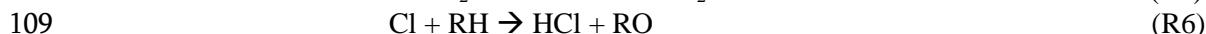
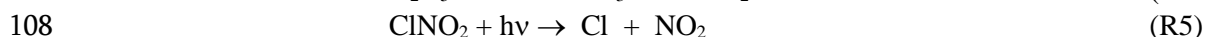
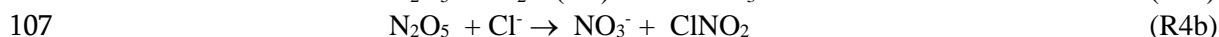
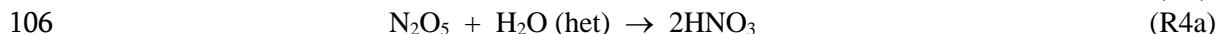
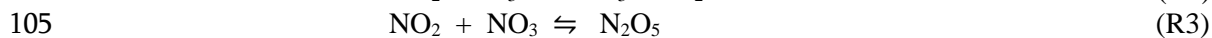


74
75 OH radicals initiate the rapid formation of multiple secondary pollutants such as O₃ and secondary
76 organic aerosols (SOA) during volatile organic compound (VOC) degradation, as well as sulfuric
77 acid and nitric acid (HNO₃) from reaction with sulfur dioxide and nitrogen dioxide (NO₂). During
78 winter, primary radical production via R1 is reduced by more than an order of magnitude due to
79 the combination of reduced sunlight and water vapor [Klonecki & Levy, 1997; Yienger et al., 1999].
80 Therefore, pollutants, such as nitrogen oxides (NO_x = NO + NO₂), VOC, and SO₂, oxidize more
81 slowly during winter and spread over wider geographic areas than during summer. The overall
82 lower radical production expected during winter suggests a higher sensitivity to the presence of less
83 common radical sources. Yet, few observational constraints of wintertime radical precursors exist
84 on scales suitable to test models of pollutant transport and transformations.

85
86 During winter, multiphase processes and direct emissions of photo-labile molecules significantly
87 influence the primary radical budget. For example, at night, nitrogen dioxide (NO₂) reacts with O₃
88 to generate the nitrate radical (NO₃), which subsequently reacts with NO₂ to form dinitrogen
89 pentoxide (N₂O₅). In winter, N₂O₅ is a major nocturnal reservoir of NO_x radicals and known to
90 react on aerosol particles, clouds, and ground surfaces, but not in the gas-phase. Aerosol particles
91 often have significant liquid water, catalyzing the hydrolysis of N₂O₅ to two HNO₃ molecules,
92 thereby limiting the lifetime of NO_x and impacting PM_{2.5} and acid deposition through subsequent
93 gas-particle partitioning of HNO₃ to form particulate nitrate (pNO₃⁻) or deposition of HNO₃ to the
94 ground [Platt and Heintz, 1994; Richards, 1983; Dentener and Crutzen, 1993; Smith et al., 1995;
95 Alexander et al., 2009;]. In particles with sufficient chloride content (pCl⁻), N₂O₅ will react
96 predominantly to form nitryl chloride and pNO₃⁻ [Finlayson-Pitts et al., 1989; Behnke & Zetzsch,
97 1990; Zetzsch & Behnke, 1992]. During the morning hours, ClNO₂ undergoes photolysis
98 recycling NO_x, increasing its lifetime and transport from source regions, while also releasing
99 highly reactive chlorine radicals (Cl), which initiate the oxidation of hydrocarbons as fast or even
100 10 to 100 times faster than OH [Orlando et al., 2003; Platt & Hönninger, 2003; Simpson et al.,

101 2015]. N₂O₅ that does not react overnight quickly becomes NO_x during the subsequent day due to
102 NO₃ radical photochemistry.

103



110

111 Utilizing the NSF/NCAR C-130 aircraft during the WINTER campaign, simultaneous airborne
112 observations of all components involved in the conversion of NO_x to N₂O₅ and its corresponding
113 multiphase reactants and products were made (See Figure 1 and supplemental information, SI).
114 Mixing ratios of speciated nitrogen oxides measured by mass spectrometry including ClNO₂,
115 N₂O₅, HNO₃, and nitrous acid (HONO), together with NO and NO₂ measured by
116 chemiluminescence (Figure 1, top panels) explain the independently measured sum total reactive
117 nitrogen abundance (NO_y= NO_x + 2* N₂O₅ +ClNO₂ +HNO₃ +HONO + ...) at all points along the
118 flight track (Figure 1, bottom). Westerly winds export NO_x emissions from the polluted urban
119 corridor of the Northeast U.S. into the marine boundary layer (MBL) over the Atlantic Ocean.
120 Over the course of a winter night, our observations show that ~25-50% of NO_x is converted to
121 N₂O₅, much of which reacts in the MBL to form HNO₃ and ClNO₂ (see SI).

122

123 Using the suite of *in situ* observations, we can directly assess the importance of each radical
124 source to the oxidative capacity of the wintertime atmosphere (See SI for details). An example set
125 of results from such calculations is shown in Figure 1 (c). We use observed nighttime
126 concentrations of O₃, humidity, ClNO₂, formaldehyde (HCHO), and HONO together with
127 modeled photolysis frequencies to calculate the total integrated concentration of radicals that
128 would be produced by these precursors over the following day. Other radical sources, such as
129 from alkene ozonolysis or dihalogen photolysis were small on a regional basis during WINTER
130 (see SI). While the nocturnal atmosphere near the surface over land is poorly mixed (See SI),
131 vertical profiling provided by the aircraft allowed us to uniquely assess the vertical extent of these
132 radical precursors. As expected, we found that over relatively warmer water in the MBL, air is
133 relatively well mixed up to 800-1500 m altitude (e.g. Figure 2), allowing more straightforward
134 calculations of radical budgets from measured concentrations.

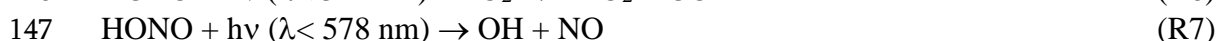
135

136 As pollution is transported offshore overnight, and ClNO₂ formation continues, we find that
137 ClNO₂ photolysis (R5) becomes the single largest source of radical oxidants. The latest pollution
138 intercept occurred before midnight local time, and several more hours of N₂O₅ production and
139 multiphase chemistry could be expected. Estimates of N₂O₅ reactivity on aerosol particles and
140 ClNO₂ yield derived from *in situ* observations [McDuffie et al., 2018a; McDuffie et al., 2018b;]
141 suggest ClNO₂ concentrations would have continued to increase overnight, accounting for as
142 much as 80% of the daytime radical source the next day.

143

144 Other important observed radical sources are O₃ via R1, HCHO via R6 and HONO via R7.

145



148

149 HCHO photolysis leads to the net formation of two HO₂ radicals, which rapidly cycle to OH in
150 the presence of NO. Annual HCHO sources are dominated by *in situ* VOC oxidation, but during
151 winter, negligible biogenic emissions of isoprene [Goldstein et al., 1998; Luecken et al., 2012;],
152 and overall lower radical concentrations, reduce the secondary production of HCHO. HCHO is
153 directly emitted from a variety of anthropogenic activities, e.g. inefficient combustion and
154 manufacturing processes [Sigsby et al., 1987; Altshuller, 1993; Anderson et al., 1996; Kelly et al.,
155 1999], but with currently uncertain magnitudes and spatial distributions. The GEOS-Chem global
156 transport model underestimates the observed WINTER HCHO by a factor of 2 on average (see
157 SI). Increasing the direct anthropogenic emission of HCHO in the model by a factor of 5 brings
158 the model into good agreement with the observations, with approximately half the HCHO in the
159 model arising from secondary oxidation of anthropogenic VOC and half from direct emissions.
160 Increasing the emissions of anthropogenic VOC that react on an hour timescale to produce
161 HCHO instead of direct emissions of HCHO would also be consistent with the observations,
162 though appropriate observational constraints are lacking. There is strong evidence that emissions
163 of HCHO and related oxygenated VOC from automobiles are significantly higher in the
164 wintertime due to the inefficient combustion associated with cold engine starts [Anderson et al.,
165 1994; Anderson et al., 1996; Li et al., 2010; Clairotte et al., 2013]. Moreover, the observed
166 HCHO is strongly correlated with tracers of fossil fuel and wood combustion (See SI). While
167 smaller than the summertime HCHO sources from biogenic VOC degradation [Fortems-Cheiney
168 et al., 2012; Luecken et al., 2012; Wolfe et al., 2016;], the wintertime anthropogenic emissions of
169 HCHO or its precursors that we infer are very important to the regional source of radicals.

170
171 HONO is both directly emitted from combustion [Kirchstetter et al., 1996; Stutz et al., 2002;],
172 and formed *in situ* from multiphase chemistry of NO₂ as well as pNO₃⁻ photolysis [Kleffmann,
173 2007; Zhou et al., 2011;]. Figure 1 shows that the measured nighttime HONO concentrations are
174 a small contributor to the primary daytime radical source over the surveyed domain. HONO is
175 more important near the urban areas, very close to the surface (<100 m), and more generally
176 enhanced over land than in the MBL (see SI). Our observations suggest a smaller role for HONO
177 on a regional basis in the daily integrated radical budget than might be inferred from ground-
178 based observations due to the poorly mixed nocturnal atmosphere [Febo et al., 1996; Stutz et al.,
179 2002; Wong et al., 2012]. However, the estimates in Figure 1 neglect a potential source from
180 pNO₃⁻ photolysis, which we assess below.

181
182 The above estimates of daytime radical sources shown in Figure 1 evolve as expected at sunrise
183 as shown in Figure 2. A stalled high-pressure system offshore of New Jersey allowed us a unique
184 opportunity to make multiple transects throughout the morning (Figure 2a) of pollution from the
185 greater New York City area that had aged overnight in the MBL (see SI). As the sun rose during
186 the flight, vertical profiles (Figure 2b) conducted along various segments revealed that the
187 instantaneous radical source from ClNO₂ photolysis was 60-80% of the total primary radical
188 source throughout the entire MBL. The importance of ClNO₂ as a radical source decreased
189 substantially at altitudes above the MBL, while that of O₃ via R1 increased as expected given the
190 steep gradients in ClNO₂ precursors (NO_x and aerosol particles) between the polluted boundary
191 layer and overlying free troposphere. The observed instantaneous production rate of radicals
192 from ClNO₂ was a factor of 5 to 10 larger than the other radical sources throughout the morning
193 as the aircraft made multiple intercepts of the pollution plume. HONO photolysis was the next
194 largest instantaneous radical source, in part due to its larger photolysis rate coefficient compared
195 to HCHO. Nighttime N₂O₅ chemistry is a removal mechanism for O₃ (R2-R4) [Platt et al., 1984;
196 Brown et al., 2004] and as such O₃ mixing ratios are often suppressed in NO_x-rich air masses
197 during the night and morning [Stutz et al., 2004], which contributes in part to the negligible
198 instantaneous source of radicals from R1 in the polluted MBL. The aircraft returned to its base
199 (segment E, Figure 2A) by flying above the MBL, where we find that the background

200 tropospheric source of radicals is dominated by that from O₃ photolysis (R1), consistent with
201 expectations.

202
203 We extend this instantaneous observational analysis during this flight using the Framework for 0-
204 D Atmospheric Modeling (F0AM) (Wolfe et al., 2016), which is based on the master chemical
205 mechanism version 3.3.1 that explicitly tracks over 5800 chemical species in over 17,000
206 reactions (Bloss et al., 2005; Jenkin et al., 1997, 2003; Saunders et al., 2003) by performing two
207 simulations; one including and one excluding reactions from chlorine and heterogeneous N₂O₅
208 formation described in Riedel et al., (2014). Initializing F0AM with WINTER measurements of
209 VOCs and inorganic gas phase species (see SI for details), Figure 3 shows the radical budget
210 occurring the day following our interception of the maximum ClNO₂ concentration observed,
211 which occurred on this flight at 6:40am in Figure 2c at point D in Figure 2a. Consistent with our
212 observational analysis, the F0AM predicted instantaneous radical production rate from ClNO₂
213 was a factor of 5 to 12 larger than the other largest radical source throughout the morning, shown
214 in Figure 3. Excluding reactions involving chlorine in F0AM caused an underestimate in the
215 integrated daily radical budget the following day of 1.8 ppbv, or a factor of 3.75. This
216 underestimate occurs primarily from excluding the early morning source of Cl radicals from
217 ClNO₂ photolysis, but also from a 114% enhancement (0.62 ppbv) in the integrated daily
218 [HCHO] that occurred because of an increase in VOC oxidation by those Cl radicals (see SI), and
219 an increase in the daily integrated ozone production of 4.7 ppbv, thereby increasing the local
220 source of OH from O₃ photolysis. These results highlight the importance of nocturnal
221 heterogeneous chlorine chemistry in coupling the secondary oxidation of VOCs, NO_y and HO_x
222 cycling, in the overall predicted daily radical budget within the WINTER domain.

223
224 We conducted 13 research flights, equally covering daytime and nighttime conditions, over land
225 and the ocean, throughout the eastern U.S. domain (see Figure 1). Applying the above
226 instantaneous radical source analysis to the wider set of flights illustrates the major importance of
227 HCHO and ClNO₂ as radical precursors, with both being more important in polluted air,
228 represented by increasing NO_x mixing ratios as shown in Figure 4. These results illustrate the
229 control of wintertime radical sources by anthropogenic emissions of NO_x and VOC, and
230 subsequent multiphase chemistry, with > 70% of the radical source stemming not from the
231 canonical reaction R1, but from ClNO₂, HCHO, and HONO photolysis. Daytime observations
232 underestimate the overall contributions of HONO and ClNO₂ to the total primary radical source
233 because both species photolyze rapidly and may not be reformed until night. Over land, this effect
234 causes an approximately 10% underestimate of the daily radical source from ClNO₂.

235
236 More over, recent studies suggest photolysis of pNO₃⁻ may be an important daytime HONO
237 source, which would not be captured by our strictly observational approach. If daytime
238 production of HONO from pNO₃⁻ photolysis occurs at the seasonally adjusted rate recently
239 suggested from summertime observations [Ye et al., 2016;], and which our observations do not
240 contradict (see SI), then HONO photolysis integrated over the day would increase the total radical
241 source shown in Figure 4 by ~50% over land, with smaller but non-negligible contributions in the
242 polluted MBL (See SI). Thus, the primary radical budget during winter may well be larger, with
243 even stronger connection to anthropogenic pollution and atypical radical sources than indicated
244 by our conservative estimate shown in Figure 4.

245
246 HCHO emissions and the multiphase chemistry of nitrogen oxides that produces ClNO₂, pNO₃⁻,
247 and HONO, are highly parameterized components of air quality or chemistry climate models, if
248 included at all [Behnke et al., 1997; Perice et al., 1998; Evans & Jacob et al., 2005; Riemer et al.,
249 2003; Anttila et al., 2006; Guenther et al., 2006; Davis et al., 2008; Bertram & Thornton, 2009;
250 Griffiths et al., 2009; Roberts et al., 2009; Vinken et al., 2011; Barkley et al., 2012; Ryder et al.,

251 2015;]. Incorporating only ClNO₂ and HCHO sources consistent with the observations from the
252 WINTER campaign into the GEOS-Chem model of global atmospheric chemistry and transport,
253 we find significant impacts on climate and air quality quantities. For example, PM_{2.5} components,
254 such as SOA and sulfate increase, while nitrate decreases (see SI), and NO_x shifts further into its
255 labile reservoirs, such as peroxy acetyl nitrate (PAN, see Figure 5). These changes are driven by
256 subsequent increased concentrations of oxidant initiators such as HO_x (OH + HO₂) radicals,
257 which increase by 40-80% over the WINTER domain from increased HCHO photolysis and VOC
258 + Cl reactions, with concomitant increases in ozone production (see SI).

259

260 Wintertime sulfate is often underestimated by air quality models, while pNO₃⁻ and nitrate
261 deposition over land have been overestimated [Tesche et al., 2002; Heald et al., 2012; Walker et
262 al., 2012; Gao et al., 2016;]. Additionally, the split between primary and secondary OA remains
263 poorly tested on a regional basis during winter [Fuzzi et al., 2006; Jimenez et al., 2009;]. The
264 increases in regional radical oxidants and changes to NO_x multiphase chemistry implied by our
265 observations reduce such discrepancies and uncertainties. Moreover, these changes halve model
266 underestimates (from 30% to 15% bias) of total peroxy nitrates (such as PAN) measured during
267 WINTER, providing additional support for increased oxidation initiated by atypical radical
268 sources, and increased export of NO_x reservoirs to the global free troposphere.

269

270 We have shown that anthropogenic emissions of NO_x and of HCHO and its analogues exert
271 control over the primary source of radical oxidants in polluted air during winter. In the case of
272 HCHO, the dormant wintertime biosphere strongly implies its wintertime sources are dominated
273 by anthropogenic emissions, which are likely enhanced due to inefficient combustion, such as
274 during vehicular cold-starts and residential wood smoke. In the case of NO_x, the natural shift
275 towards nocturnal multi-phase processing and an availability of sea-spray derived particulate
276 chloride allowed the first observational confirmation that its conversion to ClNO₂ represents a
277 critically important wintertime radical source throughout the polluted MBL that also serves to
278 enhance [HCHO]. A daytime source of HONO from pNO₃⁻ photolysis, where the pNO₃⁻
279 enhancements stem from multi-phase processing of NO_x emissions would only increase the
280 importance of local and regional anthropogenic emissions over the wintertime radical budget.

281

282 The coupling of NO_x emissions, multiphase conversion to pNO₃⁻ and ClNO₂, and subsequent
283 pNO₃⁻ photolysis to HONO represent a potentially dominant source of radicals in polluted
284 wintertime air. These insights lead to predictions of increased PM_{2.5} and increased export of NO_x
285 to the remote troposphere via PAN, where short-lived greenhouse gases such as O₃ and CH₄ are
286 far more sensitive to its presence [Singh et al., 1981; Roberts et al., 1990]. Other regions of the
287 world, such as China, Europe, and northern India also experience high NO_x, VOC sources from
288 inefficient combustion and reactive chlorine during winter [Sarwar et al., 2014; Lowe et al., 2015;
289 Li et al., 2016;]. Our findings therefore suggest important global scale revisions to our
290 understanding of wintertime pollution transformations, transport and deposition.

291

292

293

294

295

296

297

298

299

300

301

302 **References**

303

304 Alexander, B., Hastings, M. G., Allman, D. J., Dachs, J., Thornton, J. A., & Kunasek, S. A.
305 (2009). Quantifying atmospheric nitrate formation pathways based on a global model of the
306 oxygen isotopic composition ($\Delta^{17}\text{O}$) of atmospheric nitrate. *Atmos. Chem. Phys.*,
307 9(14), 5043–5056. <https://doi.org/10.5194/acp-9-5043-2009>

308

309 Altshuller, A. P. (1993). Production of aldehydes as primary emissions and from secondary
310 atmospheric reactions of alkenes and alkanes during the night and early morning hours.
311 *Atmospheric Environment. Part A. General Topics*, 27(1), 21–32.
312 [https://doi.org/https://doi.org/10.1016/0960-1686\(93\)90067-9](https://doi.org/https://doi.org/10.1016/0960-1686(93)90067-9)

313

314 Anderson, L. G., Lanning, J. A., Barrell, R., Miyagishima, J., Jones, R. H., & Wolfe, P. (1996).
315 Sources and sinks of formaldehyde and acetaldehyde: An analysis of Denver's ambient
316 concentration data. *Atmospheric Environment*, 30(12), 2113–2123.
317 [https://doi.org/https://doi.org/10.1016/1352-2310\(95\)00175-1](https://doi.org/https://doi.org/10.1016/1352-2310(95)00175-1)

318

319 Anderson, L. G., Wolfe, P., Barrell, R. A., & Lanning, J. A. (1994). The effects of oxygenated
320 fuels on the atmospheric concentrations of carbon monoxide and aldehydes in Colorado. In
321 F. . Sterrett (Ed.), *Alternative Fuesl and the Environment* (pp. 75–103). Boca Raton,
322 Florida: Lewis Publishers.

323

324 Anttila, T., Kiendler-Scharr, A., Tillmann, R., & Mentel, T. F. (2006). On the Reactive Uptake of
325 Gaseous Compounds by Organic-Coated Aqueous Aerosols: Theoretical Analysis and
326 Application to the Heterogeneous Hydrolysis of N_2O_5 . *The Journal of Physical Chemistry*
327 *A*, 110(35), 10435–10443. <https://doi.org/10.1021/jp062403c>

328

329 Barkley, M. P., Kurosu, T. P., Chance, K., De Smedt, I., Van Roozendaal, M., Arneth, A., ...
330 Guenther, A. (2012). Assessing sources of uncertainty in formaldehyde air mass factors over
331 tropical South America: Implications for top-down isoprene emission estimates. *Journal of*
332 *Geophysical Research: Atmospheres*, 117(D13). <https://doi.org/10.1029/2011JD016827>

333

334 Behnke, W., & Zetzsch, C. (1990). Heterogeneous photochemical formation of Cl atoms from
335 NaCl aerosol, NO_x and ozone. *Journal of Aerosol Science*, 21, S229–S232.
336 [https://doi.org/https://doi.org/10.1016/0021-8502\(90\)90226-N](https://doi.org/https://doi.org/10.1016/0021-8502(90)90226-N)

337

338 Behnke, W., George, C., Scheer, V., & Zetzsch, C. (1997). Production and decay of ClNO_2 from
339 the reaction of gaseous N_2O_5 with NaCl solution: Bulk and aerosol experiments. *Journal of*
340 *Geophysical Research: Atmospheres*, 102(D3), 3795–3804.
341 <https://doi.org/10.1029/96JD03057>

342

343 Bertram, T. H., & Thornton, J. A. (2009). Toward a general parameterization of N_2O_5 reactivity
344 on aqueous particles: the competing effects of particle liquid water, nitrate and chloride.
345 *Atmos. Chem. Phys.*, 9(21), 8351–8363. <https://doi.org/10.5194/acp-9-8351-2009>

346

347 Brown, S. S., Dibb, J. E., Stark, H., Aldener, M., Vozella, M., Whitlow, S., ... Ravishankara, A.
348 R. (2004). Nighttime removal of NO_x in the summer marine boundary layer. *Geophysical*
349 *Research Letters*, 31(7). <https://doi.org/10.1029/2004GL019412>

350

351 Clairotte, M., Adam, T. W., Zardini, A. A., Manfredi, U., Martini, G., Krasenbrink, A., ...
352 Astorga, C. (2013). Effects of low temperature on the cold start gaseous emissions from

353 light duty vehicles fuelled by ethanol-blended gasoline. *Applied Energy*, 102, 44–54.
354 <https://doi.org/https://doi.org/10.1016/j.apenergy.2012.08.010>
355

356 Collins, W. J., Derwent, R. G., Johnson, C. E., & Stevenson, D. S. (2002). The Oxidation of
357 Organic Compounds in the Troposphere and their Global Warming Potentials. *Climatic*
358 *Change*, 52(4), 453–479. <https://doi.org/10.1023/A:1014221225434>
359

360 Committee on Aldehydes: National Research Council. (1981). *Formaldehyde and other*
361 *aldehydes*. (N. Grossblatt, Ed.). Washington, D.C.: National Academy Press.
362

363 Dabdub, D., Meng, Z., & Seinfeld, J. H. (1997). Chemical bonding between atmospheric ozone
364 and particulate matter. *Science*, 276, 116+. Retrieved from
365 [http://link.galegroup.com/apps/doc/A19628485/AONE?u=wash_main&sid=AONE&xid=5e](http://link.galegroup.com/apps/doc/A19628485/AONE?u=wash_main&sid=AONE&xid=5eb5f24d)
366 [b5f24d](http://link.galegroup.com/apps/doc/A19628485/AONE?u=wash_main&sid=AONE&xid=5eb5f24d)
367

368 Davis, J. M., Bhave, P. V., & Foley, K. M. (2008). Parameterization of N₂O₅ reaction probabilities
369 on the surface of particles containing ammonium, sulfate, and nitrate. *Atmos. Chem. Phys.*,
370 8(17), 5295–5311. <https://doi.org/10.5194/acp-8-5295-2008>
371

372 Dentener, F. J., & Crutzen, P. J. (1993). Reaction of N₂O₅ on tropospheric aerosols: Impact on
373 the global distributions of NO_x, O₃, and OH. *Journal of Geophysical Research:*
374 *Atmospheres*, 98(D4), 7149–7163. <https://doi.org/10.1029/92JD02979>
375

376 Evans, M. J., & Jacob, D. J. (2005). Impact of new laboratory studies of N₂O₅ hydrolysis on
377 global model budgets of tropospheric nitrogen oxides, ozone, and OH. *Geophysical*
378 *Research Letters*, 32(9). <https://doi.org/10.1029/2005GL022469>
379

380 Febo, A., Perrino, C., & Allegrini, I. (1996). Measurement of nitrous acid in milan, italy, by doas
381 and diffusion denuders. *Atmospheric Environment*, 30(21), 3599–3609.
382 [https://doi.org/https://doi.org/10.1016/1352-2310\(96\)00069-6](https://doi.org/https://doi.org/10.1016/1352-2310(96)00069-6)
383

384 Finlayson-Pitts, B. J., Ezell, M. J., & Pitts, J. N. (1989). Formation of chemically active chlorine
385 compounds by reactions of atmospheric NaCl particles with gaseous N₂O₅ and ClONO₂.
386 *Nature*, 337(6204), 241–244. <http://dx.doi.org/10.1038/337241a0>
387

388 Fishman, J., Ramanathan, V., Crutzen, P. J., & Liu, S. C. (1979). Tropospheric ozone and
389 climate. *Nature*, 282(5741), 818–820. <https://doi.org/10.1038/282818a0>
390

391 Fortems-Cheiney, A., Chevallier, F., Pison, I., Bousquet, P., Saunois, M., Szopa, S., ... Fried, A.
392 (2012). The formaldehyde budget as seen by a global-scale multi-constraint and multi-
393 species inversion system. *Atmos. Chem. Phys.*, 12(15), 6699–6721.
394 <https://doi.org/10.5194/acp-12-6699-2012>
395

396 Fuzzi, S., Andreae, M. O., Huebert, B. J., Kulmala, M., Bond, T. C., Boy, M., ... Pöschl, U.
397 (2006). Critical assessment of the current state of scientific knowledge, terminology, and
398 research needs concerning the role of organic aerosols in the atmosphere, climate, and
399 global change. *Atmos. Chem. Phys.*, 6(7), 2017–2038. [https://doi.org/10.5194/acp-6-2017-](https://doi.org/10.5194/acp-6-2017-2006)
400 [2006](https://doi.org/10.5194/acp-6-2017-2006)
401

402 Gao, M., Carmichael, G. R., Wang, Y., Ji, D., Liu, Z., & Wang, Z. (2016). Improving simulations
403 of sulfate aerosols during winter haze over Northern China: the impacts of heterogeneous

404 oxidation by NO₂. *Frontiers of Environmental Science & Engineering*, 10(5), 16.
405 <https://doi.org/10.1007/s11783-016-0878-2>
406
407 Goldstein, A. H., Goulden, M. L., Munger, J. W., Wofsy, S. C., & Geron, C. D. (1998). Seasonal
408 course of isoprene emissions from a midlatitude deciduous forest. *Journal of Geophysical*
409 *Research: Atmospheres*, 103(D23), 31045–31056. <https://doi.org/10.1029/98JD02708>
410
411 Greaver, T. L., Sullivan, T. J., Herrick, J. D., Barber, M. C., Baron, J. S., Cosby, B. J., ... Novak,
412 K. J. (2012). Ecological effects of nitrogen and sulfur air pollution in the US: what do we
413 know? *Frontiers in Ecology and the Environment*, 10(7), 365–372.
414 <https://doi.org/10.1890/110049>
415
416 Griffiths, P. T., Badger, C. L., Cox, R. A., Folkers, M., Henk, H. H., & Mentel, T. F. (2009).
417 Reactive Uptake of N₂O₅ by Aerosols Containing Dicarboxylic Acids. Effect of Particle
418 Phase, Composition, and Nitrate Content. *The Journal of Physical Chemistry A*, 113(17),
419 5082–5090. <https://doi.org/10.1021/jp8096814>
420
421 Guenther, A., Karl, T., Harley, P., Wiedinmyer, C., Palmer, P. I., & Geron, C. (2006). Estimates
422 of global terrestrial isoprene emissions using MEGAN (Model of Emissions of Gases and
423 Aerosols from Nature). *Atmos. Chem. Phys.*, 6(11), 3181–3210. [https://doi.org/10.5194/acp-](https://doi.org/10.5194/acp-6-3181-2006)
424 [6-3181-2006](https://doi.org/10.5194/acp-6-3181-2006)
425
426 Heald, C. L., Collett Jr., J. L., Lee, T., Benedict, K. B., Schwandner, F. M., Li, Y., ... Pye, H. O.
427 T. (2012). Atmospheric ammonia and particulate inorganic nitrogen over the United States.
428 *Atmos. Chem. Phys.*, 12(21), 10295–10312. <https://doi.org/10.5194/acp-12-10295-2012>
429
430 Irwin, J. G., & Williams, M. L. (1988). Acid rain: Chemistry and transport. *Environmental*
431 *Pollution*, 50(1), 29–59. [https://doi.org/https://doi.org/10.1016/0269-7491\(88\)90184-4](https://doi.org/https://doi.org/10.1016/0269-7491(88)90184-4)
432
433 Jacob, D. J., & Winner, D. A. (2009). Effect of climate change on air quality. *Atmospheric*
434 *Environment*, 43(1), 51–63. <https://doi.org/https://doi.org/10.1016/j.atmosenv.2008.09.051>
435
436 Jacobson, M. C., Hansson, H.-C., Noone, K. J., & Charlson, R. J. (2000). Organic atmospheric
437 aerosols: Review and state of the science. *Reviews of Geophysics*, 38(2), 267–294.
438 <https://doi.org/10.1029/1998RG000045>
439
440 Jimenez, J. L., Canagaratna, M. R., Donahue, N. M., Prevot, A. S. H., Zhang, Q., Kroll, J. H., ...
441 Worsnop, D. R. (2009). Evolution of Organic Aerosols in the Atmosphere. *Science*,
442 326(5959), 1525 LP-1529. <https://doi.org/10.1126/science.1180353>
443
444 Kelly, T. J., Smith, D. L., & Satola, J. (1999). Emission Rates of Formaldehyde from Materials
445 and Consumer Products Found in California Homes. *Environmental Science & Technology*,
446 33(1), 81–88. <https://doi.org/10.1021/es980592+>
447
448 Kirchstetter, T. W., Harley, R. A., & Littlejohn, D. (1996). Measurement of Nitrous Acid in
449 Motor Vehicle Exhaust. *Environmental Science & Technology*, 30(9), 2843–2849.
450 <https://doi.org/10.1021/es960135y>
451
452 Kleffmann, J. (2007). Daytime Sources of Nitrous Acid (HONO) in the Atmospheric Boundary
453 Layer. *ChemPhysChem*, 8(8), 1137–1144. <https://doi.org/10.1002/cphc.200700016>
454

455 Klonecki, A., & Levy II, H. (1997). Tropospheric chemical ozone tendencies in CO-CH₄-NO_y-
456 H₂O system: Their sensitivity to variations in environmental parameters and their
457 application to a global chemistry transport model study. *Journal of Geophysical Research:*
458 *Atmospheres*, 102(D17), 21221–21237. <https://doi.org/10.1029/97JD01805>
459

460 Levy II, H., Mahlman, J. D., Moxim, W. J., & Liu, S. C. (1985). Tropospheric ozone: The role of
461 transport. *Journal of Geophysical Research: Atmospheres*, 90(D2), 3753–3772.
462 <https://doi.org/10.1029/JD090iD02p03753>
463

464 Levy, H. (1971). Normal Atmosphere: Large Radical and Formaldehyde Concentrations
465 Predicted. *Science*, 173(3992), 141 LP-143. <https://doi.org/10.1126/science.173.3992.141>
466

467 Li, J., Gong, C., Wang, E., Yu, X., Wang, Z., & Liu, X. (2010). Emissions of Formaldehyde and
468 Unburned Methanol from a Spark-Ignition Methanol Engine during Cold Start. *Energy &*
469 *Fuels*, 24(2), 863–870. <https://doi.org/10.1021/ef9009982>
470

471 Li, Q., Zhang, L., Wang, T., Tham, Y. J., Ahmadov, R., Xue, L., ... Zheng, J. (2016). Impacts of
472 heterogeneous uptake of dinitrogen pentoxide and chlorine activation on ozone and reactive
473 nitrogen partitioning: improvement and application of the WRF-Chem model in southern
474 China. *Atmos. Chem. Phys.*, 16(23), 14875–14890. [https://doi.org/10.5194/acp-16-14875-
475 2016](https://doi.org/10.5194/acp-16-14875-2016)
476

477 Lowe, D., Archer-Nicholls, S., Morgan, W., Allan, J., Utembe, S., Ouyang, B., ... McFiggans, G.
478 (2015). WRF-Chem model predictions of the regional impacts of N₂O₅ heterogeneous
479 processes on night-time chemistry over north-western Europe. *Atmos. Chem. Phys.*, 15(3),
480 1385–1409. <https://doi.org/10.5194/acp-15-1385-2015>
481

482 Luecken, D. J., Hutzell, W. T., Strum, M. L., & Pouliot, G. A. (2012). Regional sources of
483 atmospheric formaldehyde and acetaldehyde, and implications for atmospheric modeling.
484 *Atmospheric Environment*, 47, 477–490.
485 <https://doi.org/https://doi.org/10.1016/j.atmosenv.2011.10.005>
486

487 McDuffie, E. E., Fibiger, D. L., Dubé, W. P., Lopez Hilfiker, F., Lee, B. H., Jaeglé, L., ... Brown,
488 S. S. (2018). ClNO₂ Yields From Aircraft Measurements During the 2015 WINTER
489 Campaign and Critical Evaluation of the Current Parameterization. *Journal of Geophysical*
490 *Research: Atmospheres*, 123(22), 12,15,913-994. <https://doi.org/10.1029/2018JD029358>
491

492 McDuffie, E. E., Fibiger, D. L., Dubé, W. P., Lopez-Hilfiker, F., Lee, B. H., Thornton, J. A., ...
493 Brown, S. S. (2018). Heterogeneous N₂O₅ Uptake During Winter: Aircraft Measurements
494 During the 2015 WINTER Campaign and Critical Evaluation of Current Parameterizations.
495 *Journal of Geophysical Research: Atmospheres*, 123(8), 4345–4372.
496 <https://doi.org/10.1002/2018JD028336>
497

498 Menz, F. C., & Seip, H. M. (2004). Acid rain in Europe and the United States: an update.
499 *Environmental Science & Policy*, 7(4), 253–265.
500 <https://doi.org/https://doi.org/10.1016/j.envsci.2004.05.005>
501

502 Orlando, J. J., Tyndall, G. S., Apel, E. C., Riemer, D. D., & Paulson, S. E. (2003). Rate
503 coefficients and mechanisms of the reaction of Cl-atoms with a series of unsaturated
504 hydrocarbons under atmospheric conditions. *International Journal of Chemical Kinetics*,
505 35(8), 334–353. <https://doi.org/10.1002/kin.10135>

506
507 Peirce, T., Geron, C., Bender, L., Dennis, R., Tonnesen, G., & Guenther, A. (1998). Influence of
508 increased isoprene emissions on regional ozone modeling. *Journal of Geophysical*
509 *Research: Atmospheres*, 103(D19), 25611–25629. <https://doi.org/10.1029/98JD01804>
510
511 Platt, U., & Hönninger, G. (2003). The role of halogen species in the troposphere. *Chemosphere*,
512 52(2), 325–338. [https://doi.org/https://doi.org/10.1016/S0045-6535\(03\)00216-9](https://doi.org/https://doi.org/10.1016/S0045-6535(03)00216-9)
513
514 Platt, U. F., Winer, A. M., Biermann, H. W., Atkinson, R., & Pitts, J. N. (1984). Measurement of
515 nitrate radical concentrations in continental air. *Environmental Science & Technology*,
516 18(5), 365–369. <https://doi.org/10.1021/es00123a015>
517
518 Platt, U., & Heintz, F. (1994). Nitrate Radicals in Tropospheric Chemistry. *Israel Journal of*
519 *Chemistry*, 34(3-4), 289–300. <https://doi.org/10.1002/ijch.199400033>
520
521 Ramanathan, V., & Feng, Y. (2009). Air pollution, greenhouse gases and climate change: Global
522 and regional perspectives. *Atmospheric Environment*, 43(1), 37–50.
523 <https://doi.org/https://doi.org/10.1016/j.atmosenv.2008.09.063>
524
525 Richards, L. W. (1983). Comments on the oxidation of NO₂ to nitrate—day and night.
526 *Atmospheric Environment (1967)*, 17(2), 397–402.
527 [https://doi.org/https://doi.org/10.1016/0004-6981\(83\)90057-4](https://doi.org/https://doi.org/10.1016/0004-6981(83)90057-4)
528
529 Riedel, T. P., Wolfe, G. M., Danas, K. T., Gilman, J. B., Kuster, W. C., Bon, D. M., ... Thornton,
530 J. a. (2014). An MCM modeling study of nitryl chloride (ClNO₂) impacts on oxidation,
531 ozone production and nitrogen oxide partitioning in polluted continental outflow.
532 *Atmospheric Chemistry and Physics*, 14(8), 3789–3800. [https://doi.org/10.5194/acp-14-](https://doi.org/10.5194/acp-14-3789-2014)
533 [3789-2014](https://doi.org/10.5194/acp-14-3789-2014)
534
535 Roberts, J. M. (1990). The atmospheric chemistry of organic nitrates. *Atmospheric Environment*.
536 *Part A. General Topics*, 24(2), 243–287. [https://doi.org/https://doi.org/10.1016/0960-](https://doi.org/https://doi.org/10.1016/0960-1686(90)90108-Y)
537 [1686\(90\)90108-Y](https://doi.org/10.1016/0960-1686(90)90108-Y)
538
539 Roberts, J. M., Osthoff, H. D., Brown, S. S., Ravishankara, A. R., Coffman, D., Quinn, P., &
540 Bates, T. (2009). Laboratory studies of products of N₂O₅ uptake on Cl⁻ containing
541 substrates. *Geophysical Research Letters*, 36(20). <https://doi.org/10.1029/2009GL040448>
542
543 Ryder, O. S., Campbell, N. R., Shaloski, M., Al-Mashat, H., Nathanson, G. M., & Bertram, T. H.
544 (2015). Role of Organics in Regulating ClNO₂ Production at the Air–Sea Interface. *The*
545 *Journal of Physical Chemistry A*, 119(31), 8519–8526. <https://doi.org/10.1021/jp5129673>
546
547 Sarwar, G., Simon, H., Xing, J., & Mathur, R. (2014). Importance of tropospheric ClNO₂
548 chemistry across the Northern Hemisphere. *Geophysical Research Letters*, 41(11), 4050–
549 4058. <https://doi.org/10.1002/2014GL059962>
550
551 Schofield, C. L. (1976). Acid Precipitation: Effects on Fish. *Ambio*, 5(5/6), 228–230. Retrieved
552 from <http://www.jstor.org/stable/4312222>
553
554 Seinfeld, J. H. (1989). Urban Air Pollution: State of the Science. *Science*, 243(4892), 745–752.
555 <https://doi.org/10.1126/science.243.4892.745>
556

557 Shepson, P. B., Hastie, D. R., So, K. W., Schiff, H. I., & Wong, P. (1992). Relationships between
558 PAN, PPN and O₃ at urban and rural sites in Ontario. *Atmospheric Environment. Part A.*
559 *General Topics*, 26(7), 1259–1270. [https://doi.org/https://doi.org/10.1016/0960-](https://doi.org/https://doi.org/10.1016/0960-1686(92)90387-Z)
560 [1686\(92\)90387-Z](https://doi.org/https://doi.org/10.1016/0960-1686(92)90387-Z)
561
562 Sigsby, J. E., Tejada, S., Ray, W., Lang, J. M., & Duncan, J. W. (1987). Volatile organic
563 compound emissions from 46 in-use passenger cars. *Environmental Science & Technology*,
564 21(5), 466–475. <https://doi.org/10.1021/es00159a007>
565
566 Singh, H. B., & Hanst, P. L. (1981). Peroxyacetyl nitrate (PAN) in the unpolluted atmosphere: An
567 important reservoir for nitrogen oxides. *Geophysical Research Letters*, 8(8), 941–944.
568 <https://doi.org/10.1029/GL008i008p00941>
569
570 Smith, N., Plane, J. M. C., Nien, C.-F., & Solomon, P. A. (1995). Nighttime radical chemistry in
571 the San Joaquin Valley. *Atmospheric Environment*, 29(21), 2887–2897.
572 [https://doi.org/https://doi.org/10.1016/1352-2310\(95\)00032-T](https://doi.org/https://doi.org/10.1016/1352-2310(95)00032-T)
573
574 Stutz, J., Alicke, B., Ackermann, R., Geyer, A., White, A., & Williams, E. (2004). Vertical
575 profiles of NO₃, N₂O₅, O₃, and NO_x in the nocturnal boundary layer: 1. Observations
576 during the Texas Air Quality Study 2000. *Journal of Geophysical Research: Atmospheres*,
577 109(D12). <https://doi.org/10.1029/2003JD004209>
578
579 Stutz, J., Alicke, B., & Neftel, A. (2002). Nitrous acid formation in the urban atmosphere:
580 Gradient measurements of NO₂ and HONO over grass in Milan, Italy. *Journal of*
581 *Geophysical Research: Atmospheres*, 107(D22), LOP 5-1-LOP 5-15.
582 <https://doi.org/10.1029/2001JD000390>
583
584 Tesche, T. W., Morris, R., Tonnesen, G., McNally, D., Boylan, J., & Brewer, P. (2006).
585 CMAQ/CAMx annual 2002 performance evaluation over the eastern US. *Atmospheric*
586 *Environment*, 40(26), 4906–4919.
587 <https://doi.org/https://doi.org/10.1016/j.atmosenv.2005.08.046>
588
589 Vinken, G. C. M., Boersma, K. F., Jacob, D. J., & Meijer, E. W. (2011). Accounting for non-
590 linear chemistry of ship plumes in the GEOS-Chem global chemistry transport model.
591 *Atmos. Chem. Phys.*, 11(22), 11707–11722. <https://doi.org/10.5194/acp-11-11707-2011>
592
593 Volkamer, R., Jimenez, J. L., San Martini, F., Dzepina, K., Zhang, Q., Salcedo, D., ... Molina, M.
594 J. (2006). Secondary organic aerosol formation from anthropogenic air pollution: Rapid and
595 higher than expected. *Geophysical Research Letters*, 33(17).
596 <https://doi.org/10.1029/2006GL026899>
597
598 Walker, J. M., Philip, S., Martin, R. V., & Seinfeld, J. H. (2012). Simulation of nitrate, sulfate,
599 and ammonium aerosols over the United States. *Atmos. Chem. Phys.*, 12(22), 11213–11227.
600 <https://doi.org/10.5194/acp-12-11213-2012>
601
602 Wang, W. C., Yung, Y. L., Lacis, A. A., Mo, T., & Hansen, J. E. (1976). Greenhouse Effects due
603 to Man-Made Perturbations of Trace Gases. *Science*, 194(4266), 685 LP-690.
604 <https://doi.org/10.1126/science.194.4266.685>
605
606 Weinstock, B. (1969). Carbon Monoxide: Residence Time in the Atmosphere. *Science*,
607 166(3902), 224 LP-225. <https://doi.org/10.1126/science.166.3902.224>

608
609 Wert, B. P., Trainer, M., Fried, A., Ryerson, T. B., Henry, B., Potter, W., ... Wisthaler, A. (2003).
610 Signatures of terminal alkene oxidation in airborne formaldehyde measurements during
611 TexAQS 2000. *Journal of Geophysical Research: Atmospheres*, 108(D3).
612 <https://doi.org/10.1029/2002JD002502>
613
614 Wolfe, G. M., Kaiser, J., Hanisco, T. F., Keutsch, F. N., de Gouw, J. A., Gilman, J. B., ...
615 Warneke, C. (2016). Formaldehyde production from isoprene oxidation
616 across NO_x regimes. *Atmos. Chem. Phys.*, 16(4), 2597–2610. [https://doi.org/10.5194/acp-](https://doi.org/10.5194/acp-16-2597-2016)
617 [16-2597-2016](https://doi.org/10.5194/acp-16-2597-2016)
618
619 Wolfe, G. M., Marvin, M. R., Roberts, S. J., Travis, K. R., & Liao, J. (2016). The Framework for
620 0-D Atmospheric Modeling (F0AM) v3.1. *Geosci. Model Dev.*, 9(9), 3309–3319.
621 <https://doi.org/10.5194/gmd-9-3309-2016>
622
623 Wong, K. W., Tsai, C., Lefer, B., Haman, C., Grossberg, N., Brune, W. H., ... Stutz, J. (2012).
624 Daytime HONO vertical gradients during SHARP 2009 in Houston, TX. *Atmos. Chem.*
625 *Phys.*, 12(2), 635–652. <https://doi.org/10.5194/acp-12-635-2012>
626
627 Ye, C., Zhou, X., Pu, D., Stutz, J., Festa, J., Spolaor, M., ... Knote, C. (2016). Rapid cycling of
628 reactive nitrogen in the marine boundary layer. *Nature*, 532, 489. Retrieved from
629 <https://doi.org/10.1038/nature17195>
630
631 Yienger, J. J. (1999). Correction to “An evaluation of chemistry’s role in the winter-spring ozone
632 maximum found in the northern midlatitude free troposphere” by J. J. Yienger et al. *Journal*
633 *of Geophysical Research*, 104(D7), 8329.
634 Zetzsch, C., & Behnke, W. (1992). Heterogeneous Photochemical Sources of Atomic Cl in the
635 Troposphere. *Berichte Der Bunsengesellschaft Für Physikalische Chemie*, 96(3), 488–493.
636 <https://doi.org/10.1002/bbpc.19920960351>
637
638 Zhou, X., Zhang, N., TerAvest, M., Tang, D., Hou, J., Bertman, S., ... Stevens, P. S. (2011).
639 Nitric acid photolysis on forest canopy surface as a source for tropospheric nitrous acid.
640 *Nature Geoscience*, 4, 440. Retrieved from <https://doi.org/10.1038/ngeo1164>

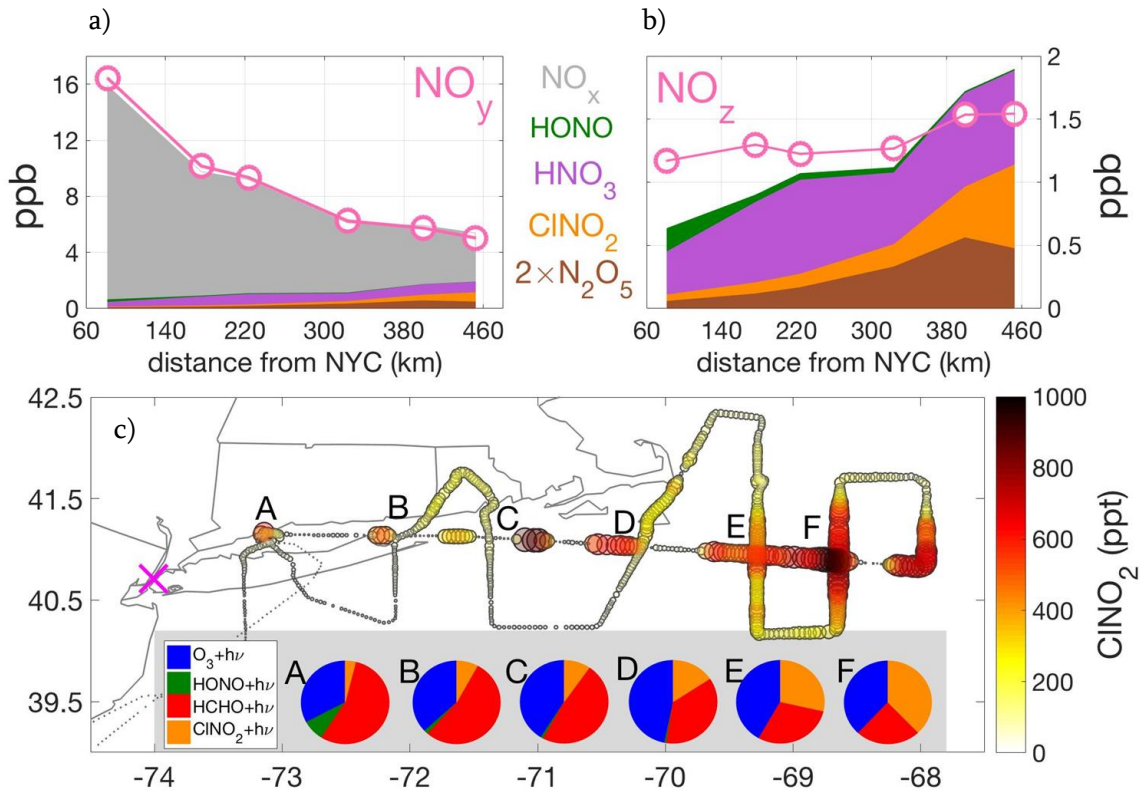


Figure 1. Top panels: evolution of nitrogen oxide reservoirs downwind of New York City observed aboard the NSF/NCAR C-130 aircraft during Research Flight 3 (RF; February 7, 2015) of the WINTER campaign. Observations are from below 2 km altitude only, and correspond to 7pm to 11pm local time. NO_y represents the sum of all forms of oxidized nitrogen that can be converted to NO at high temperatures (a) NO_z represents the sum of all oxidized nitrogen species except for NO_x ($\text{NO} + \text{NO}_2$) and is derived from the measured $\text{NO}_y - \text{NO}_x$ (b). The gap between total NO_z and the sum of individual components that occurs near to NYC, while within the total calibration uncertainty of the sum, can likely be explained by a combination of pNO_3^- and peroxy nitrates (see SI). (c) map of the flight track colored and sized by the measured mixing ratio of ClNO_2 . The nearly straight trajectory between points A through F consisted of periodic ascents and descents of the aircraft between 500 and 2000 m altitude, profiling the vertical extent of the polluted atmospheric boundary layer. Pie charts show the observationally constrained contributions of different radical precursors to the integrated daytime radical source (see text).

642
 643
 644
 645
 646
 647
 648
 649
 650
 651
 652
 653
 654
 655
 656
 657
 658
 659
 660
 661
 662
 663
 664
 665

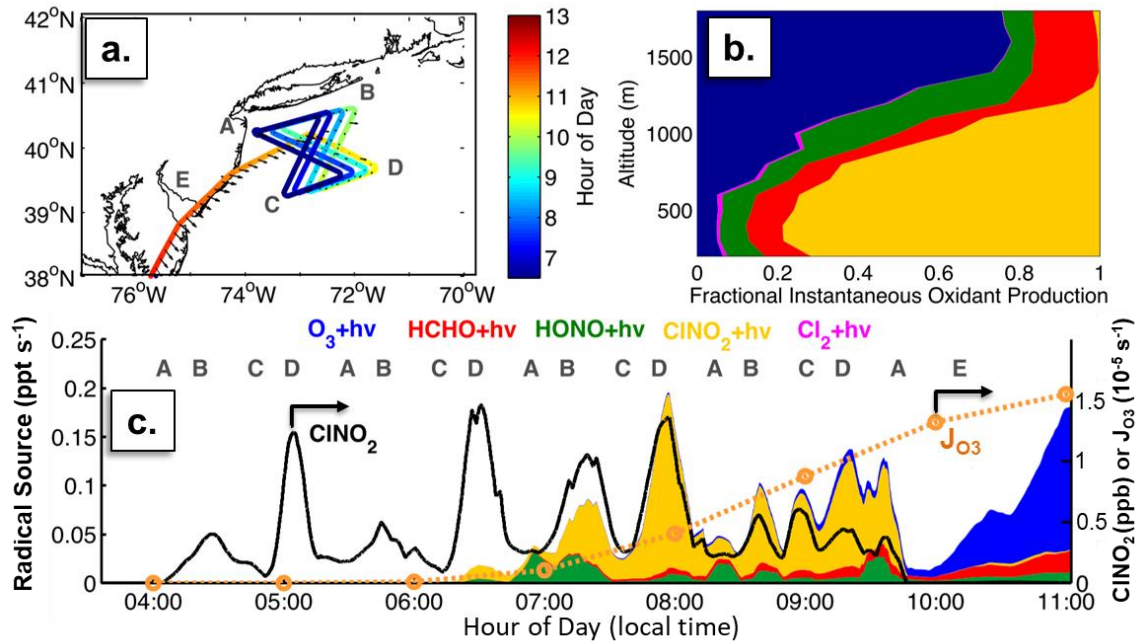


Figure 2. (a) Flight track of the NSF/NCAR C-130 on Research Flight 8 of the WINTER campaign, colored by local time of day. Sunrise occurred at approximately 6:30 AM local time. Only portions with altitudes <2000 m are shown. (b) Vertical profiles of the instantaneous radical source calculated from observations of solar radiation and radical precursors. (c) Time series of the instantaneous radical source (left axis, stacked color), CINO₂ mixing ratios (right axis, ppb), and the O₃ photolysis frequency (orange circles, right axis, 10⁻⁵ s⁻¹)

666
667
668
669
670
671
672
673
674
675
676
677
678
679
680
681
682
683
684
685
686
687
688
689
690
691
692
693

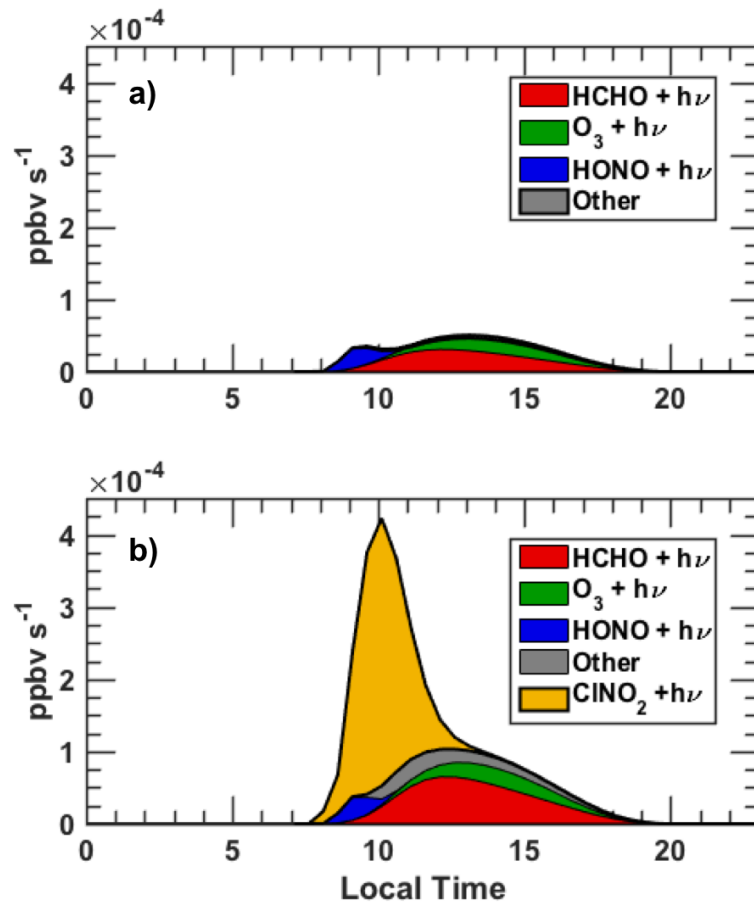


Figure 3. Summary of daily, net primary radical production rates calculated the day following our interception of the peak ClNO₂ concentrations in RF08 using the FOAM box model initialized with WINTER observations without including chlorine reactions (a) and including chlorine reactions (b).

694
 695
 696
 697
 698
 699
 700
 701
 702
 703
 704
 705
 706
 707
 708
 709
 710
 711
 712
 713
 714
 715
 716
 717
 718
 719
 720

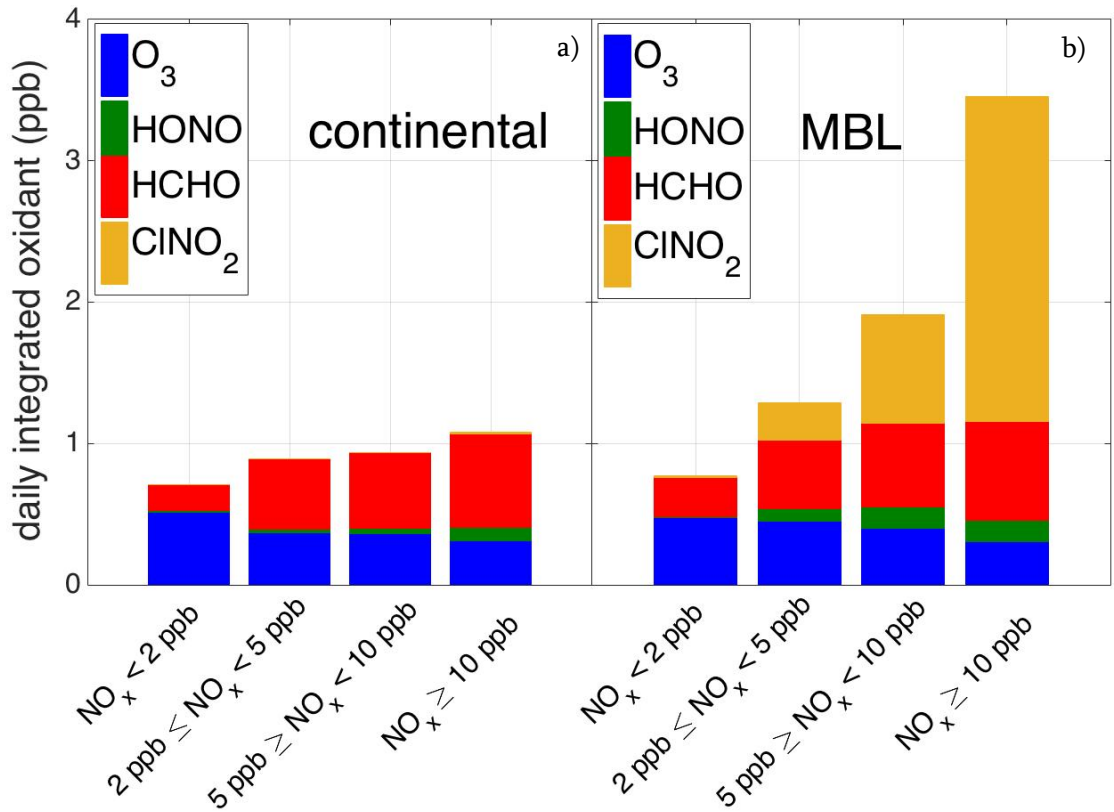


Figure 4. Summary of daily primary radical source calculated from observations of O_3 , H_2O_2 , ClNO_2 , HONO, and HCHO made during the daytime in the continental boundary layer (a), and at night within the MBL (b). Data are binned as a function of observed NO_x mixing ratios with lower values indicating less polluted air and higher values indicating more polluted air. In the left pane, we show only daytime observations over land, as these better reflect a well-mixed polluted boundary layer. For comparison, we show estimates based on nighttime observations within the MBL in the right panel. These two regimes are a fair representation of the typical importance of each radical source over the entire data set. See SI for additional statistics and calculations).

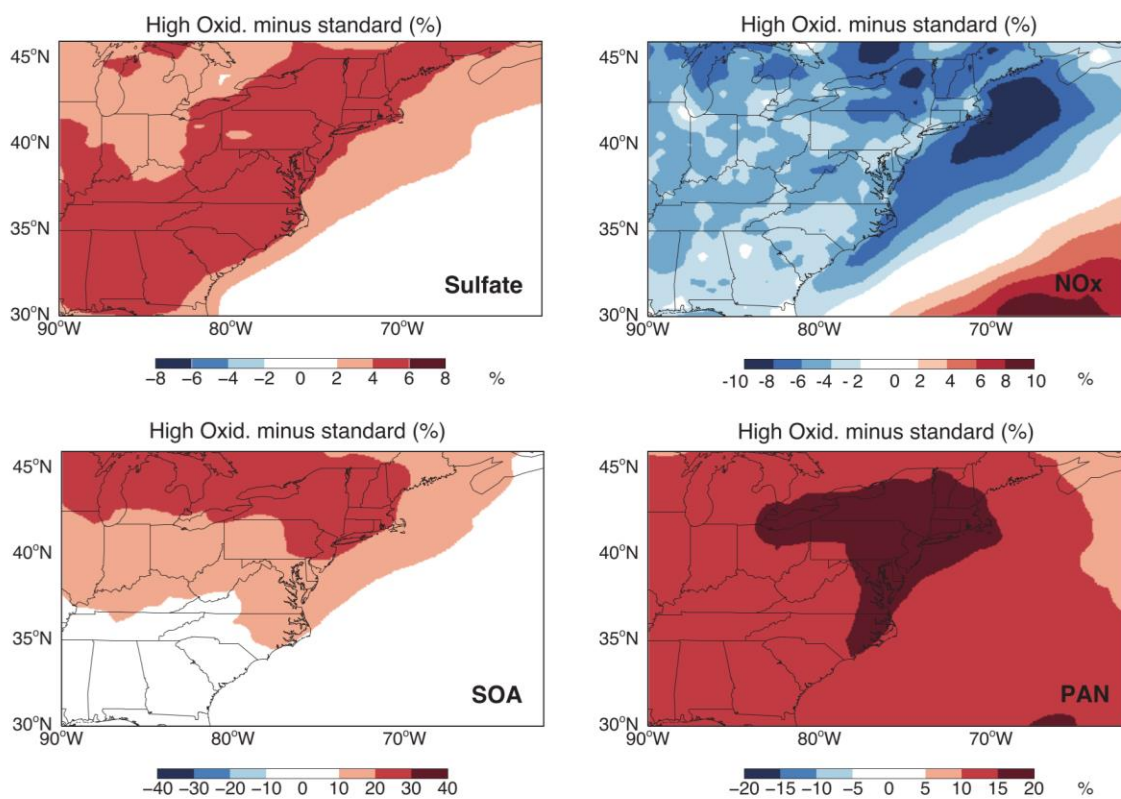


Figure 5. Relative changes in GEOS-Chem model predicted sulfate, SOA, NO_x and PAN abundances between runs using standard emissions and chemistry, and those using updated emissions of HCHO and CINO₂ chemistry based on the WINTER observations. Enhanced oxidative capacity in the boundary layer from enhanced HCHO (over land) and CINO₂ (in the MBL) leads to increased conversion of SO₂ to sulfate aerosol mass, VOC to secondary organic aerosol mass, and increased conversion of NO_x into reservoirs such as PAN which in turn affects its global distribution.

721
722